Intravitreal Injection of Proinsulin-Loaded Microspheres Delays Photoreceptor Cell Death and Vision Loss in the *rd10* Mouse Model of Retinitis Pigmentosa

Carolina Isiegas,[1] Jorge A. Marinich-Madzarevich,[1] Miguel Marchena,[2] José M. Ruiz,[1] María J. Cano,[1] Pedro de la Villa,[2] Catalina Hernández-Sánchez,[3,4] Enrique J. de la Rosa,[4] and Flora de Pablo[3,4]

[1]ProRetina Therapeutics, S.L., Noain, Spain
[2]Department of System Biology, School of Medicine, Universidad de Alcalá de Henares, Madrid, Spain
[3]Centro de Investigación Biomédica en Red de Diabetes y Enfermedades Metabólicas Asociadas (CIBERDEM), ISCIII, Madrid, Spain
[4]3D Lab, Development, Differentiation & Degeneration, Centro de Investigaciones Biológicas, Consejo Superior de Investigaciones Científicas (CIB/CSIC), Madrid, Spain

Correspondence: Flora de Pablo, 3D Lab, Development, Differentiation & Degeneration, Centro de Investigaciones Biológicas, Consejo Superior de Investigaciones Científicas (CIB/CSIC), Ramiro de Maeztu 9, 28040, Madrid, Spain;
fdepablo@cib.csic.es.
Enrique J. de la Rosa, 3D Lab, Development, Differentiation & Degeneration, Centro de Investigaciones Biológicas, Consejo Superior de Investigaciones Científicas (CIB/CSIC), Ramiro de Maeztu 9, 28040, Madrid, Spain;
ejdelarosa@cib.csic.es.

Submitted: February 5, 2016
Accepted: June 1, 2016

Citation: Isiegas C, Marinich-Madzarevich JA, Marchena M, et al. Intravitreal injection of proinsulin-loaded microspheres delays photoreceptor cell death and vision loss in the *rd10* mouse model of retinitis pigmentosa. *Invest Ophthalmol Vis Sci.* 2016;57:3610–3618. DOI:10.1167/iovs.16-19300

Purpose. The induction of proinsulin expression by transgenesis or intramuscular gene therapy has been shown previously to retard retinal degeneration in mouse and rat models of retinitis pigmentosa (RP), a group of inherited conditions that result in visual impairment. We investigated whether intraocular treatment with biodegradable poly (lactic-co-glycolic) acid microspheres (PLGA-MS) loaded with proinsulin has cellular and functional neuroprotective effects in the retina.

Methods. Experiments were performed using the *Pde6b*^{rd10} mouse model of RP. Methionylated human recombinant proinsulin (hPI) was formulated in PLGA-MS, which were administered by intravitreal injection on postnatal days (P) 14 to 15. Retinal neuroprotection was assessed at P25 by electroretinography, and by evaluating outer nuclear layer (ONL) cellular preservation. The attenuation of photoreceptor cell death by hPI was determined by TUNEL assay in cultured P22 retinas, as well as Akt phosphorylation by immunoblotting.

Results. We successfully formulated hPI PLGA-MS to deliver the active molecule for several weeks in vitro. The amplitude of b-cone and mixed b-waves in electroretinographic recording was significantly higher in eyes injected with hPI-PLGA-MS compared to control eyes. Treatment with hPI-PLGA-MS attenuated photoreceptor cell loss, as revealed by comparing ONL thickness and the number of cell rows in this layer in treated versus untreated retinas. Finally, hPI prevented photoreceptor cell death and increased Akt^{Thr308} phosphorylation in organotypic cultured retinas.

Conclusions. Retinal degeneration in the *rd10* mouse was slowed by a single intravitreal injection of hPI-PLGA-MS. Human recombinant proinsulin elicited a rapid and effective neuroprotective effect when administered in biodegradable microspheres, which may constitute a future potentially feasible delivery method for proinsulin-based treatment of RP.

Keywords: retinitis pigmentosa, neuroprotection, photoreceptors

Inherited retinal dystrophies, including retinitis pigmentosa (RP), are a large group of diseases in which over 250 genes and loci have been implicated (available in the public domain at http://www.sph.uth.tmc.edu/Retnet/disease.htm). This genetic diversity underscores the need to develop alternative therapeutic approaches to attenuate disease progression while gene therapies are developed and optimized. Numerous gene mutations associated with RP, as well as other retinal dystrophies, have been shown to induce photoreceptor cell death, leading to progressive loss of visual function.[1–4] Among other RP models, this pathologic process has been widely studied in the *rd10* mouse, which carries an autosomal recessive, missense mutation in the *Pde6b* gene.[1,5] The disease course in this model[6,7] allows for evaluation of experimental treatments by electroretinographic and histologic analysis.

Promoting cell survival is a plausible strategy for the treatment of various retinal dystrophies. Over 2 decades ago, Faktorovitch et al.[8] first proposed that growth factors could be used to treat retinal degenerative diseases. Of the many factors tested in initial studies, in which the ability to rescue photoreceptors from the damaging effect of light was assessed, seven showed promise, including fibroblast growth factor (FGF), human ciliary neurotrophic factor (CNTF), and insulin-like growth factor II (IGF-II).[9] Subsequent studies investigated the use of peptides and growth factors in different animal models of eye diseases, including neurotrophins 3 and 4, and brain-derived neurotrophic factor (BDNF),[10] and attempted to identify appropriate minimally invasive and controlled drug delivery systems.[11–16] Compounds extensively tested include glial cell-derived neurotrophic factor (GDNF),[17] CNTF,[18] and,

more recently, rod-derived cone viability factor (RdCVF).[19] Interestingly, the steroid sex hormone progesterone also has been identified as a promising candidate to decrease cell death in the *rd1* mouse model.[20] Research has begun to unravel the antiapoptotic mechanism of progesterone action, which appears to involve the progesterone receptor membrane component 1 (PGRMC1), the expression of which is upregulated in the degenerating *rd10* mouse retina.[21]

Proinsulin and insulin also have shown their neuroprotective effect in several models of RP.[22–24] Long considered a mere low-activity precursor of pancreatic insulin, proinsulin is produced locally by several tissues outside the pancreas, and has been shown to significantly attenuate cell death during neural development (see review[25–28]). The therapeutic potential of human proinsulin (hPI) has been demonstrated in studies that have systemically increased hPI levels. In the *rd10* mouse, low-level constitutive transgenic expression of hPI in muscle attenuates vision loss and delays photoreceptor cell death.[22] However, the use of this procedure in a clinical setting is not feasible. In the *P23H* rat model of autosomal dominant RP, hPI administered by intramuscular injection of adenoassociated viral vector, pseudotype 1 (AAV1), which is suitable for gene therapy in humans, preserves the structure and function of cones and rods, as well with their contacts with postsynaptic neurons.[24]

Although systemic gene therapy is feasible in human patients, a more convenient strategy for RP therapy is local administration close to the affected cells, which would allow sustained delivery in animal models and eventually could be applied to patients. Biocompatible, biodegradable poly (lactic-co-glycolic acid) microspheres (PLGA-MS) disappear after releasing the drug contained within, and are well tolerated following intravitreal injection in animals and humans.[29,30] The primary objective of the present study was to manufacture a suitable hPI-PLGA-MS formulation that could gradually deliver an appropriate concentration of the active molecule. Next, we set out to assess the neuroprotective effect of this formulation in vivo in the *rd10* mouse, when injected before the onset of massive photoreceptor cell death. To further examine the direct antiapoptotic effects of hPI on retina cells, we studied the changes in TUNEL staining and Akt^{Thr308} phosphorylation after hPI treatment in retinal explants from *rd10* mice.

Materials and Methods

Animals

The *rd10* mouse model of retinal degeneration is a homozygous mutant for phosphodiesterase 6b (*Pde6b*$^{rd10/rd10}$) on a C57BL/6J background. It was kindly provided by Bo Chang from The Jackson Laboratory (Bar Harbor, ME, USA). All animals were housed and handled in accordance with the ARVO Statement for the Use of Animals in Ophthalmic and Vision Research, European Union guidelines, and those of the local ethics committees of the CSIC and the Comunidad de Madrid. Mice were bred in the CIB core facilities on a 12/12-hour light/dark cycle.

PLGA Microsphere Formulation

Methionylated hPI, Batch F148510 2 1-1, was manufactured by Biotecnol Limited (Hertfordshire, UK) and PLGA-MS were manufactured by ProRetina Therapeutics S.L. (Noain, Spain). The hPI was encapsulated in microspheres at a concentration of 3.2 μg hPI/mg PLGA-MS, equivalent to 22.4 μg hPI/mL of injected material (7 mg PLGA-MS/mL). As a control, empty PLGA-MS (7 mg/mL) were injected. The vehicle used for experimental and control materials was 4% (wt/vol) mannitol, 1% (wt/vol) Tween-20, and 1% (wt/vol) carboxymethylcellulose.

Microsphere Fabrication Procedure

We generated PLGA-MS from a W1/O/W2 emulsion at room temperature and normal atmospheric pressure using the solvent evaporation technique, in a modified version of the method of Mao et al.[31] Dichloromethane (1.5 mL) was added to a test tube containing 200 mg RG503H polymer (Resomer RG 503H; Mat. Nr.: 719870; Boehringer Ingelheim, Germany). Once the oil phase was formed (O + polymer), 300 μL of aqueous phase (W1 + 5 mg/mL hPI) was added slowly, drop by drop, to avoid the formation of large drops in the oil phase. The mixture was homogenized for 1 minute and 2 mL of 2.5% (wt/vol) PVA (W2) aqueous solution was added to the vial. The contents were stirred again at low speed for 1 minute with an UltraTurrax T25 homogenizer (IKA, Staufen, Germany). The resulting W1/O/W2 emulsion was stirred for 3 hours at room temperature and normal atmospheric pressure to evaporate the organic solvent. The microspheres were washed with 900 mL of cold Milli-Q water (Merck Millipore Corporation, Billerica, MA, USA) to remove PVA from the solution and were collected over a 1-μm mesh, and gathered using a spatula. The microsphere preparation was frozen for 24 hours at −80°C and finally lyophilized for 24 hours. Microspheres were examined for particle size distribution by laser light scattering using a Coulter LS32 (Beckman Coulter, Inc., Brea, CA, USA). Particles (40 mg) then were suspended in distilled water and particle size calculated by Fraunhofer approximation.

Intravitreal Injection

Male and female mice of at least 5 g bodyweight were treated at postnatal day (P) 14 or 15. Animals were anesthetized with an intraperitoneal (IP) injection of a ketamine (95 mg/kg) + xylazine (5 mg/kg) mixture, diluted in 0.9% (wt/vol) NaCl. A Hamilton syringe (Hamilton Robotics, Bonaduz, Switzerland) with a 33-gauge (G) needle was used to intravitreally inject a single 1-μl volume of a sterile preparation of hPI-PLGA-MS (22.4 ng dose in the case of FP50) into the right eye, or an equivalent volume of control (empty) PLGA-MS into the left eye. Tobramycin (Tobrex) was applied to the eye after injection to protect the cornea and prevent infection. Electroretinographic (ERG) recordings were performed at P25. Animals then were euthanized and retinas and serum samples collected.

ERG Recording

Mice were handled and ERG recordings performed as described previously.[22] Measurements were performed by an observer blind to the experimental condition of the animal. Electroretinographic signals were amplified and band filtered between 0.3 and 1000 Hz (CP511 Preamplifier; Grass Instruments, Quincy, MA, USA) and digitized to 10 kHz using a PowerLab acquisition data card (AD Instruments Ltd., Oxfordshire, UK). Graphic representations of the signals recorded and the luminous stimuli control were performed with the Scope v6.4 PowerLab software. Electroretinographic wave amplitudes were measured off-line and the results averaged. Wave amplitude analysis was performed using the MATLAB (Mathworks, Natick, MA, USA) application.

Histology and Cell Counting

Animals were euthanized, the dorsal part of the eyeball was marked with a red label to allow orientation and then the eyes were enucleated. Eyes were fixed for 2 hours in 4% (wt/vol) paraformaldehyde in PBS, and then cryoprotected by incuba-

tion in increasing concentrations of sucrose (10%, 20%, 30%, and 40% [wt/vol] in PBS). The eyes then were embedded in Tissue-Tek (Sakura Finetec, Torrance, CA, USA), and frozen on dry ice. Cryostat sections (5 μm) were mounted on poly-lysine-coated glass slides, dried at room temperature, fixed for 15 minutes with 4% (wt/vol) paraformaldehyde in PBS, and coverslipped with Fluoroshield containing 4′,6-diamidino-2-phenylindole (DAPI; Sigma-Aldrich Corp., St. Louis, MO, USA) to counterstain the nuclei. Five μm equatorial (horizontal) sections in which optic nerve appeared were collected (the total number of sections were 20–25). Since the microinjection procedure was performed in the dorsal region, we avoided this area for quantification purposes.

Five sections per retina were analyzed. For each section, one photograph was taken for each of the six retinal zones defined as T1, T2, T3, T4, T5, and T6 along the nasotemporal retinal axis. In the nasal region, T1 was located at 100 μm from the ora serrata; T3, 100 μm from the optic nerve; and T2 equidistant from T1 and T3. The same procedure was followed in the temporal region, taking photographs T4, T5, and T6 from the optic nerve to the ora serrata.

In each photo, measurements were performed in triplicate to obtain an average value per retinal zone per section. The following parameters were measured using ImageJ v1.44p software (available in the public domain at https://imagej.nih.gov/ij; National Institutes of Health [NIH], Bethesda, MD, USA): outer nuclear layer (ONL) thickness (using the "freehand line" and "measure" tools) and number of rows in the ONL (by visually counting the nuclei). The raw data acquired were exported and pixel values for ONL thickness were converted to μm using the appropriate equivalence for the microscope used.

Statistical Analysis

The statistical analysis of histologic and ERG data was performed by independent observers. Repeated measurements for each of the six retinal regions defined for histologic evaluation were validated using the Hotelling *t*-test to identify artifacts. For histologic data, the values obtained for hPI-PLGA-MS–treated and control eyes were compared using a Student's *t*-test for paired samples. For ERG data, differences in wave amplitudes between treated and control eyes were assessed by repeated measures analysis and Student's *t*-test used for comparison. Significance was established at $P < 0.05$.

Measurement of Proinsulin Concentration

The concentration of hPI was measured in PLGA-MS supernatants and in mouse serum samples and retinal extracts. For the analysis of supernatant and serum samples, 20-μl volumes were assayed in duplicate. Retinal extracts were prepared by homogenizing one retina in 60 μL of RIPA buffer (50 mM $NaH_2PO_4.H_20$, 100 mM $Na_2HPO_4.7H_20$, 100 mM NaCl, 0.1% [wt/vol] Triton X-100, and protease inhibitors) and assaying 20-μl samples in duplicate. The total protein content of retinal extracts was determined by Bradford assay. Human proinsulin levels were measured using the Human Total Proinsulin ELISA kit (EZHPI-15K; Merck Millipore) according to the manufacturer's instructions. Plates were read using a microplate reader set to dual wavelength measurement at 450 nm with a background correction set at 590 nm. Absorbance data were analyzed using MasterPlex 2010 software (Merlin Equipment Ltd., Dorset, UK). Picomolar concentrations extrapolated from the standard curve were assessed using the acceptance criteria recommended by the manufacturer. In addition, a prevalidation study was performed using the retinal extract as the matrix, in which values were classified as follows: <10 pM, nondetectable; 10 to 20 pM, detectable but not quantifiable; >20 pM, quantifiable. For serum samples hPI levels were expressed in pM. For retina samples, detectable values were expressed as pmol per gram of total protein or as fmol per retina.

Whole Mount Retinal Cultures

Retinas were dissected from P22 *rd10* mice and retinal explants were cultured free-floating in M24 multiwell plates for 24 hours in 1.2 mL Dulbecco's modified Eagle's medium (DMEM)/F12 medium containing N2-supplement, but without insulin and, where indicated, containing 10^{-8} M hPI. Retinas were subsequently fixed in 4% (wt/vol) paraformaldehyde in PBS for 1 hour at RT and processed for detection of cell death.

Cell Death Visualization and Counting

Photoreceptor cell death was visualized by DNA fragmentation assay terminal deoxynucleotidyl transferase-mediated dUTP nick end labeling (DeadEnd FluorometricTUNEL system; Promega, Madison, WI, USA), as described previously.[22] After labeling, the retinas were flat-mounted in Fluoromount-G (Southern Biotechnology, Birmingham, AL, USA), stained with DAPI, and analyzed on a laser confocal microscope (TCS SP5; Leica, Microsystems, Wetzlar, Germany). Image acquisition was performed in 4 areas of each retina. Serial optical sections were acquired in the depth of the ONL, as determined in retinal sections, to ensure that TUNEL-positive nuclei belong to photoreceptors. Direct counting of TUNEL-positive cells was done on merged images using ImageJ v1.48.s software. Paired statistical analysis was performed using the Wilcoxon signed-rank test.

Immunoblots

Retinas were cultured as indicated above for a 3-hour period without insulin or proinsulin and then hPI (10^{-8} M) was added to the group of treated retinas, maintaining the culture for additional 2, 5, or 15 minutes. Total Akt protein and phospho-Akt^{Thr308} levels were determined by immunoblot. Protein extraction was done by sonication of the retinas in RIPA lysis buffer (containing 2 mM Na_3VO_4, 10 mM NaF, and 4 mM Na Pirophosphate as phosphatase inhibitors), maintaining the tubes 30 minutes on ice. Then, 15 μg protein of each sample were fractionated by precast 10% to 12% (wt/vol) sodium dodecyl sulfate (SDS)–polyacrylamide gel (Criterion TGX, Bio-Rad, Munich, Germany) electrophoresis, and proteins were transferred to polyvinylidine fluoride (PVDF) membranes using a Trans-Blot Turbo system (Bio-Rad Laboratories, Hercules, CA, USA). Blots were incubated with rabbit polyclonal anti-$pAkt^{Thr308}$ (1:1000; Cell Signaling, Beverly, MA, USA) and developed with the appropriate peroxidase-conjugated secondary antibody (1:20,000) using the Pierce ECL Western Blotting Substrate. After striping the membrane was incubated with rabbit polyclonal anti-Akt1 (1:1000; Cell Signaling) and developed as indicated above. Films were scanned and images were analyzed using the ImageJ v1.48.s program.

Results

Release Profile of Human Proinsulin From PLGA Microspheres

To assess the efficacy of a sustained-release hPI formulation as a neuroprotective therapy in the *rd10* mouse, we first formulated the protein in PLGA microspheres. A number of different hPI preparations encapsulated in PGLA-MS were developed and characterized to evaluate a wide range of release parameters, including initial burst, progressive release, and release interval.

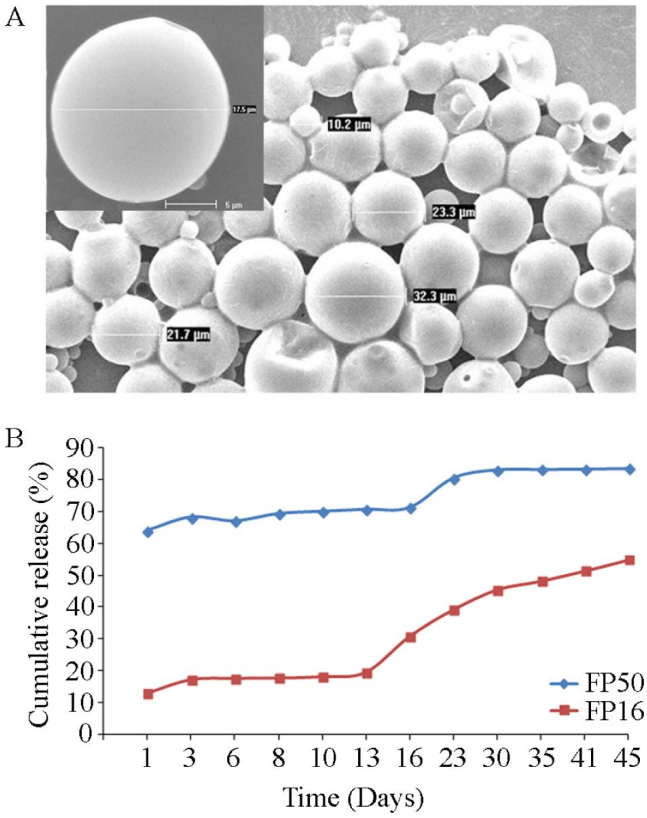

FIGURE 1. Morphology and protein release properties of hPI-PLGA microspheres. (**A**) Scanning electron microscopy microphotography of a pellet containing microspheres of different sizes. The diameter of several microspheres is indicated. The *inset* shows a single enlarged microsphere. (**B**) Cumulative release of hPI in vitro from two formulations (FP16 and FP50) for up to 45 days. The percentage of the total load released was calculated by measuring hPI levels in the medium. Note that the *x*-axis is not a linear scale.

The quality of the PLGA-MS was screened by scanning electron microscopy to assess particle size and surface characteristics. A typical pellet of PLGA-MS (Fig. 1A) included particles with a smooth surface, 10 to 32 µm in diameter, which is an adequate size for intravitreal injection. The hPI release profile varied among batches, particularly in terms of initial burst. Two different profiles, displaying a low and a high initial burst of release, are shown in Figure 1B. Due to the rapid progression of retinal degeneration in the *rd10* mouse model, we selected the FP50 formulation for the study; this formulation was characterized by a high initial burst, which was likely to ensure a therapeutic concentration within 24 hours of injection, as well as continuous in vitro release of hPI for at least 45 days.

The FP50 formulation used in the present study contained 22.42 µg hPI/mL of injected preparation. Male and female *rd10* mice at P14 or P15 (i.e., before the onset of any detectable photoreceptor death) were injected with 1 µL of FP50 in the right eye (treated) and 1 µL of empty PLGA-MS from the same batch in the left eye (control). Analysis of hPI concentration in extracts taken from treated retinas at P25 ($n = 17$) revealed considerable variation in in vivo hPI release, with values ranging from undetectable to 203 pmol/g of total protein, with most values in the range of 16 to 32 pmol/g. In control retinas, as well as in the serum, hPI always was undetectable. These results demonstrated that relatively low levels of hPI released from the intravitreal MS did reach the target tissue without systemic dissemination.

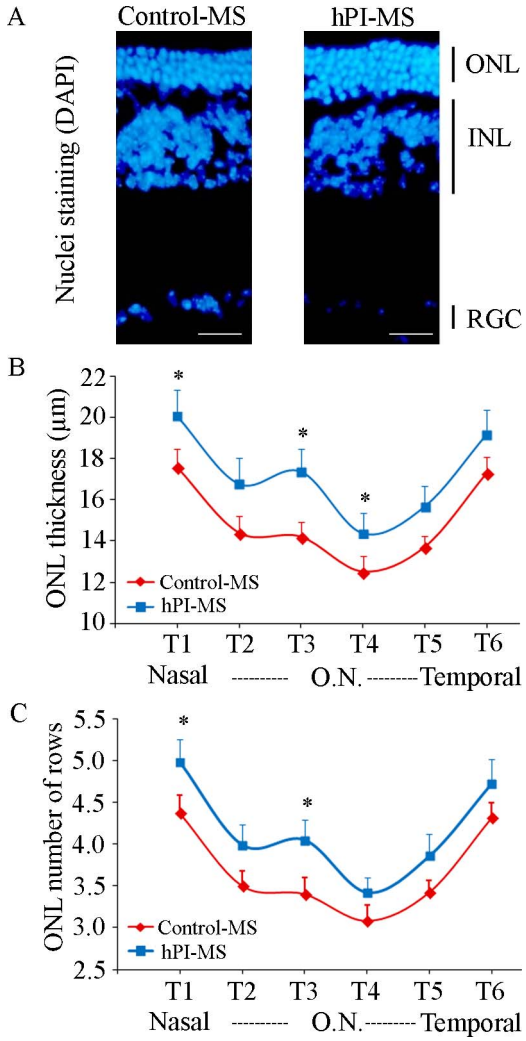

FIGURE 2. Attenuation of photoreceptor cell loss in the *rd10* mouse retina after hPI treatment. Retinal sections from control and treated eyes were processed at P25. (**A**) Representative images of DAPI-stained retinal sections from control (Control-MS) and treated (hPI-MS) retinas of the same animal. Images were taken from nasal regions, approximately equidistant between the optic nerve and the ora serrata (T2). The ONL, inner nuclear layer (INL) and retinal ganglion cells (RGC) are indicated. (**B**) After DAPI staining, ONL thickness was measured in 6 regions of the retina, in nasotemporal sequence (T1–T6), in equatorial sections (see Methods). (**C**) The number of cell rows in the ONL, which corresponds to photoreceptors, was scored in DAPI-stained retina sections, as described in (**B**). Plots show the mean (± SEM) values for control (Control-MS) and hPI-treated (hPI-MS) retinas. $n = 11$ mice, 5 sections per retina, 3 measurements per region and section; O.N., optic nerve. *$P < 0.05$. *Scale bar*: 15 µm.

Photoreceptor Preservation in the *rd10* Mouse After Intravitreal Injection of hPI-PLGA-MS

Histologic evaluation of the *rd10* retina at P25, by which time massive photoreceptor loss has occurred, revealed photoreceptor preservation in hPI-PLGA-MS–treated eyes with respect to control eyes, at least in some areas (Fig. 2). The average thickness of the ONL in treated retinas was greater than that measured in control retinas in all regions (Fig. 2B), with significant differences observed in T1 (nasal) and T3 and T4 (central) retinal regions. The number of photoreceptor rows also was higher in retinas treated with hPI-PLGA-MS compared to contralateral control retinas (Fig. 2C), with signifi-

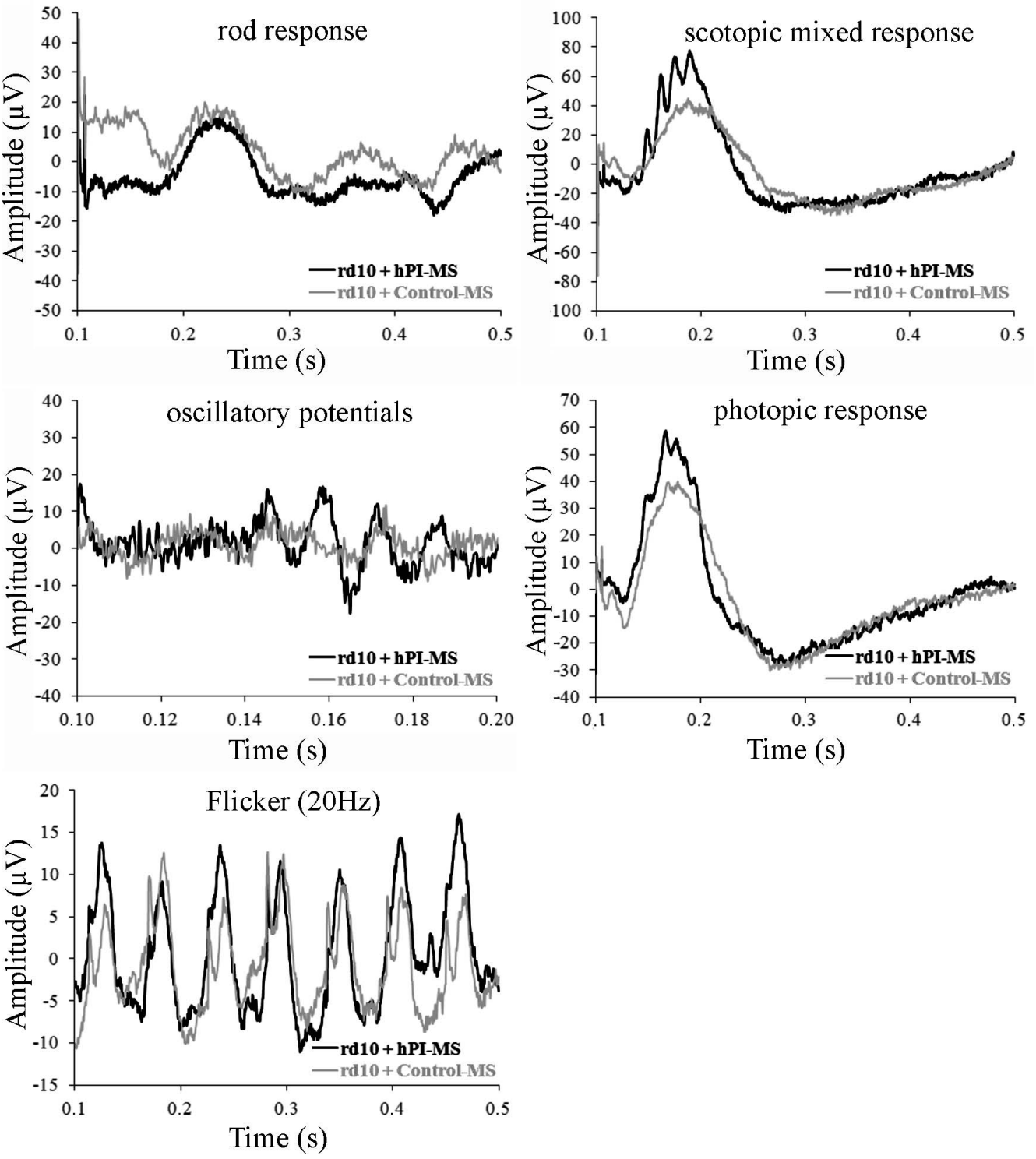

Figure 3. Preservation of ERG responses in hPI-treated *rd10* eyes compared to control eyes. A representative example of the different ERG responses recorded in hPI-treated eyes (hPI-MS) and contralateral control eyes (Control-MS) is shown. Electroretinographs were obtained at P25, and the type of response recorded is indicated in each Figure.

cant differences observed in the nasal T1 region and close to the optic nerve (T3). That the effect of hPI was more marked in the nasal retina concurs with previous findings in the *P23H* rat model.[24] There was no significant difference in the INL thickness in retinas treated with hPI-PLGA-MS compared to contralateral control retinas.

Preservation of Visual Function in *rd10* Retinas Treated With hPI-PLGA-MS

The neuroprotective effect of hPI at the functional level was evaluated by ERG in *rd10* mice at P25, in dark- and light-adapted conditions to measure rod- and cone-mediated vision, respectively. In general, ERG waves in hPI-PLGA-MS–treated eyes (Fig. 3,

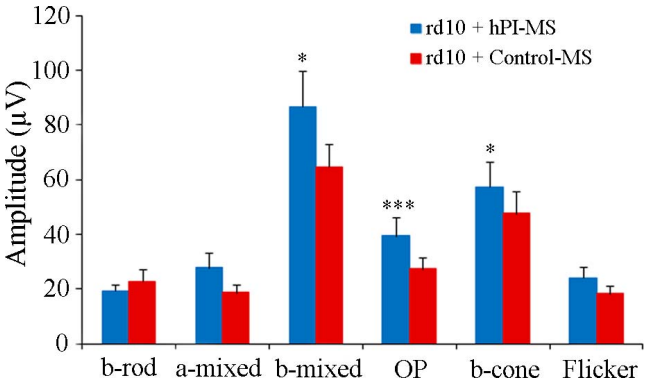

FIGURE 4. Average amplitudes of ERG waves in hPI-treated (hPI-MS) and control (Control-MS) retinas. $n = 15$ to 17 mice for different responses. *Scale bars*: mean ± SEM. $^{*}P < 0.05$, $^{***}P < 0.005$.

black lines) were better defined and greater in amplitude than in the control ones (grey lines). The average b-mixed, b-cone, and oscillatory potential (OP) amplitudes were significantly higher in hPI-treated versus control retinas (Fig. 4). Electroretinography, thus, confirmed a protective effect on a number of parameters of visual function in hPI-PLGA-MS–treated retinas, consistent with the partial preservation of the retinal structure seen in treated eyes, as described above.

Attenuation of Cell Death in Organotypic Cultures of hPI-Treated *rd10* Retinas

We performed ex vivo studies to support that hPI had a prosurvival effect on photoreceptor cells, as previously suggested by a transgenic model expressing hPI in the muscle.[22] Retinal explants were prepared from *rd10* mice at P22, before the peak of cell death, and cultured in the absence or presence of 10^{-8} M hPI. After 24 hours in culture, the number of TUNEL-positive cells detected in the photoreceptor layer was significantly lower in hPI-treated retinas compared to untreated retinas (Fig. 5), indicating a protective effect of hPI on photoreceptors.

Increase in Akt Phosphorylation in Organotypic Cultures of hPI-Treated *rd10* Retinas

The hPI signaling pathway was studied next in retinal explants. P22 retinal explants were deprived from growth factors for 3 hours and then cultured in the absence or presence of 10^{-8} M hPI for periods from 2 to 15 minutes. Phosphorylation of Akt^{Thr308} was significantly increased by hPI at all tested time points (Fig. 6). In contrast, there was no stimulation of ERK phosphorylation (data not shown). Thus, these results suggested that the neuroprotective effect of hPI is mediated by the activation of the PI3-K/Akt signaling pathway. Since this was observed in whole retina cultures, the activation of PI3-K/Akt pathway may not be occurring exclusively in photoreceptor cells, and other cell types could be implicated in this response, an aspect to be addressed in future studies.

Taken together, these data indicated that intravitreal injection of PLGA microspheres was a feasible method for the intraocular delivery of hPI, comparable to that previously achieved using a systemic approach.[22] Proinsulin, which was able to activate the PI3-K/Akt pathway and to decrease photoreceptor cell death, exerted a therapeutic effect by preserving the ONL structure as well as the electroretinographic function in the *rd10* retina.

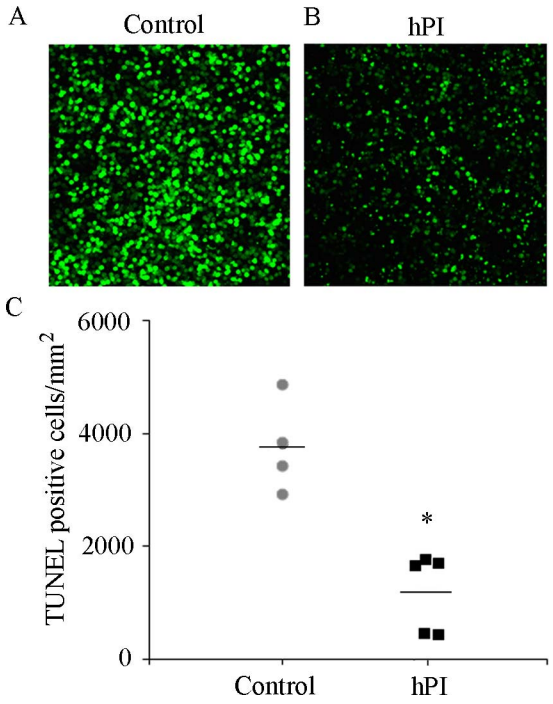

FIGURE 5. Photoreceptor cell death is ameliorated by hPI treatment in explant cultures of *rd10* retinas. Whole mount retinas from P22 *rd10* mice were cultured for 24 hours in either defined medium ([**A**], $n = 4$) or defined medium + naked hPI 10^{-8} M ([**B**], $n = 5$). TUNEL subsequently was performed and the number of individual positive cells in 4 areas of the retina was scored and plotted (**C**). *Dots* and *squares* represent values for individual retinas; *horizontal line* represents the mean value; $^{*}P < 0.05$.

DISCUSSION

The present findings demonstrated that intravitreal administration of hPI formulated in biodegradable PLGA microspheres is a feasible approach that displays cellular and electrophysiologic neuroprotective effects in the *rd10* mouse model.

The development of affordable mutation-specific therapy for RP is extremely demanding, given that this retinal dystrophy is caused by multiple diverse mutations at a large number of genetic loci, each affecting a small number of patients.[32] Accordingly, the development of neuroprotective strategies is a key area of research in the search for mutation-independent therapies for RP.[15,33] While gene augmentation or replacement therapy has been successfully applied to patients with Leber's congenital amaurosis, the resulting improvement in vision is transient, with photoreceptor degeneration ultimately progressing over time.[34,35] Neuroprotection could constitute a valuable complementary therapy, and could be applied before, in parallel with, or even after gene-specific therapy to prolong vision.

In previous proof-of-concept studies in mice and rats, we demonstrated that systemic elevation of hPI levels by transgenesis[22] or *AAV1* gene therapy[24] delays photoreceptor degeneration and prolongs visual function. An effective local administration route, if feasible, should facilitate future clinical trials. After testing several microsphere formulations of hPI, we identified a formulation (FP50) that allowed an initial rapid delivery of the active molecule, while levels of which were sustainably released in vitro for over a month (Fig. 1B). In vivo, intact hPI was detected in retinas from injected animals several days after a single intravitreal injection (data not shown). Moreover, the released hPI was biologically active and exerted

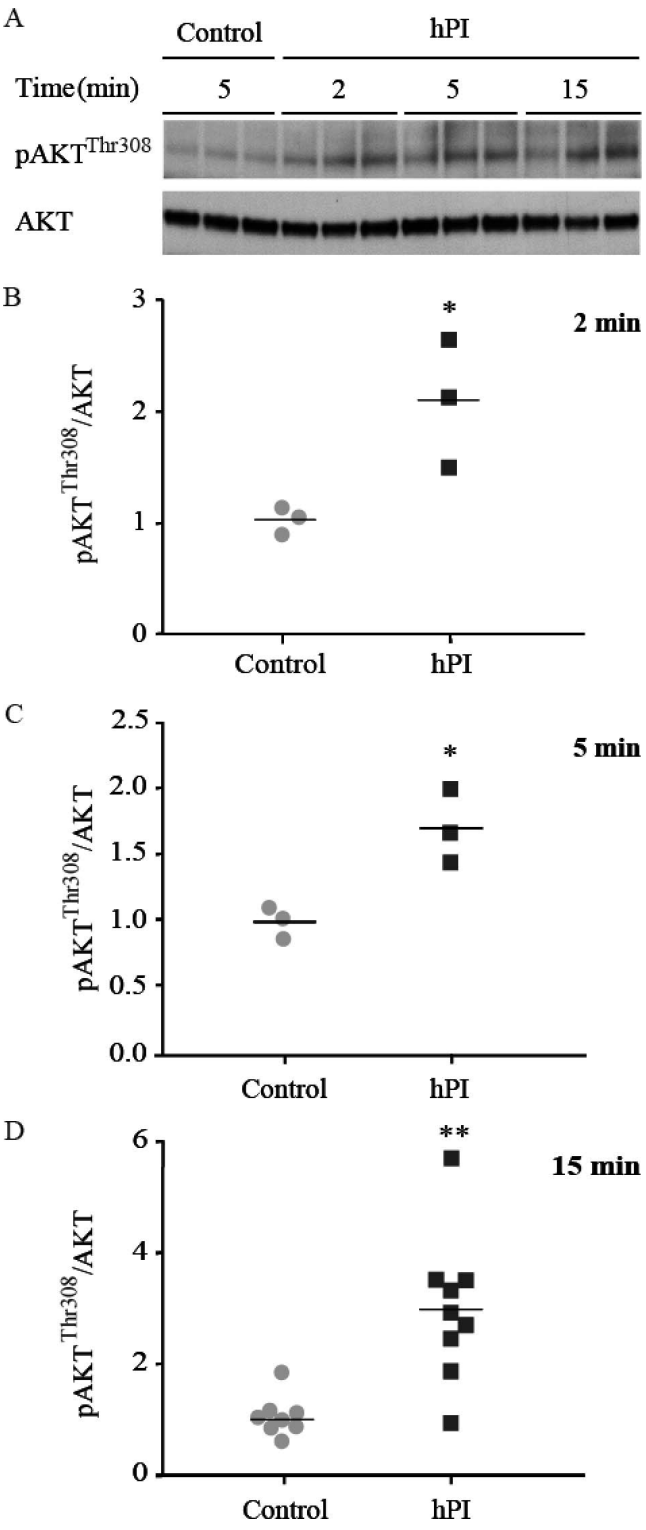

FIGURE 6. Akt phosphorylation is stimulated by hPI treatment in explant cultures of *rd10* retinas. Whole mount retinas from P22 *rd10* mice were cultured for up to 15 minutes in either defined medium (Control) or defined medium + naked 10^{-8} M hPI. Retina extracts were prepared and immunoblotted with antibodies against $pAkt^{Thr308}$ and total Akt proteins. Representative blots are shown (**A**). The ratio of the $pAkt^{Thr308}$ and total Akt signals at 2 (**B**), 5 (**C**), and 15 (**D**) minutes was obtained for individual retinas. *Dots* and *squares* represent values for individual retinas; *horizontal line* represents the mean value; $^{*}P < 0.05$, $^{**}P < 0.01$.

a therapeutic effect by preserving nasal and central retinal ONL structure as well as electroretinographic function, specifically the OP, cone, and combined rod-cone responses. We speculate that the ERG response may reflect a dual effect of hPI, that is, a reduction in rod cell death, which leads to a structural improvement in the retina, and exerts a neuroprotective effect on synapses between rods and bipolar cells that improves their functionality. The lack of an increase in the amplitude of the a-mixed wave indicates that the electric response of these photoreceptors is not increased after hPI treatment. However, if there are more photoreceptors with less degenerated synaptic terminals, one would expect improved function. At low light intensity, this effect may not be sufficient to significantly increase activation of bipolar cells. However, at high light intensity, better preserved photoreceptors and their synapses lead to the generation of a higher response in bipolar cells (higher b-mixed wave). This more efficient activation of bipolar cells, in turn, generates a stronger input in the amacrine cells, thereby resulting in the significant increase in OP after hPI treatment. This proposed explanation is supported by our previous findings in another RP model, the *P23H* rat. In that study, we found that administration of hPI via intramuscular injection of an AAV vector preserved synaptic connectivity between photoreceptors and bipolar and horizontal cells.[24]

In recent years there has been much debate about the best means of delivering exogenous proteins to the retina.[36] Intraocular implants of encapsulated cells delivering CNTF have been tested in animal models of retinal degeneration with good tolerance (reviewed previously[37]). In fact, insulin released from subconjunctivally implanted hydrogels reduced retinal DNA fragmentation in diabetic rats and these implants did not alter retinal histology over a 2-month period.[38] Our preliminary studies of local tolerance to PLGA-MS in rabbits revealed no adverse effects (data not shown). Nonetheless, further studies of the effects of intravitreal MS injections in large animals (dogs or primates) will be necessary to assess safety and efficacy of this approach. The biodegradable nature of the PLGA-MS and the short half-life of proinsulin should facilitate adequate dose-titration to ensure transient secondary effects if caused by hPI.

The efficacy of intravitreal PLGA-MS treatment described here in a model of RP represents a preliminary proof-of-concept which supports that this is a potentially feasible treatment strategy, eventually applicable in a variety of diseases of the eye, including uveitis, macular edema, retinal detachment, and age-related macular degeneration (reviewed previously[30]).

Our findings in explant cultures confirm a prosurvival effect of hPI on photoreceptors, as previously proposed based on the developmental effects of proinsulin. Whether the cells responding to hPI are exclusively the photoreceptors, or there is an additional effect on other retinal cell types that might be beneficial as well for photoreceptor function still is unclear and worth studying in the future. We have found in a previous study that another member of the insulin related family of proteins, IGF-I, has a complex effect on the *rd10* retina, involving polarization of microglia and attenuation of Müller glial cell reactive gliosis.[39,40] However, due to its high potency stimulating proliferative pathways mediated by the IGF type I receptor, IGF-I is not a good candidate for a neuroprotective treatment. Paracrine effects may be important not only to maintain the primary degenerating photoreceptor, the rods in the case of the *rd10* mutant mice, but also to rescue the secondary death affecting the cones and additional retinal cells. A similar type of neuroprotective effect also has been proposed for the action of RdCVF in degenerated retina.[19] Also a panretinal preservation of photoreceptor nuclei was found in

the *rd10* mice, at P30, in a quantitative careful analysis after treatment with tauroursodeoxycholic acid (TUDCA).[41]

While we did not specifically investigate the mechanism of action of hPI as a prosurvival molecule, the presence of type A insulin receptor (IR-A) mRNA was confirmed in wild type and *rd10* retinas (data not shown). This receptor has been found to bind proinsulin and IGF-II with high affinity. In contrast, proinsulin showed poor binding to the IR-B and it does not bind IGF type I receptors.[42] The proinsulin signaling through IR-A also was supported by the phosphorylation of Akt^{Thr308}, residue phosphorylated upon insulin and growth factor receptor stimulation. There is a large body of evidence demonstrating the presence of insulin receptors in the retina of different species.[43] In bovine and human retina these receptors are widely distributed in all retinal layers,[44,45] meaning that most cell types are sensitive to proinsulin. The presence and important role in neuroprotection of the insulin receptors in rod photoreceptor cells has been demonstrated clearly in a study using cell-specific receptor knockout mice.[46]

At least during retinal development, the prosurvival action of proinsulin has been shown to involve the activation of the PI3K pathway.[47] Moreover, in the adult mouse retina Akt activation in response to IR signaling is required to protect against light damage.[46] Regardless, further studies will be necessary to elucidate the molecular mechanisms underlying the observed prosurvival effect of hPI in the *rd10* mouse. Despite the several pending questions on proinsulin effect on the dystrophic retina, our findings underscore the potential value of MS-formulated hPI for a future RP therapy.

Acknowledgments

The authors thank the staff of the CIB animal facility and the confocal microscopy unit for technical assistance, Rocío Herrero-Vanrell for advice on the initial formulation of MS and Teresa Suárez for critical reading of the manuscript.

Supported by Grants from the Spanish Ministerio de Ciencia e Innovación (MICINN) and Spanish Ministerio de Economía y Competitividad (MINECO), SAF2010-21879 (EJdlR and PdlV), SAF2013-41059-R (FdP and EJdlR), and technical personnel support from CIBERDEM, ISCIII, Madrid, Spain.

Disclosure: **C. Isiegas**, ProRetina Therapeutics, S.L. (E, I); **J.A. Marinich-Madzarevich**, ProRetina Therapeutics, S.L (E); **M. Marchena**, ProRetina Therapeutics, S.L. (E); **J.M. Ruiz**, ProRetina Therapeutics, S.L. (E, I); **M.J. Cano**, ProRetina Therapeutics, S.L. (E, I); **P. de la Villa**, ProRetina Therapeutics, S.L. (E), P; **C. Hernández-Sánchez**, ProRetina Therapeutics, S.L. (I); **E.J. de la Rosa**, ProRetina Therapeutics, S.L. (F, I), P; **F. de Pablo**, ProRetina Therapeutics, S.L. (F, I), P

References

1. Chang GQ, Hao Y, Wong F. Apoptosis: final common pathway of photoreceptor death in rd, rds, and rhodopsin mutant mice. *Neuron*. 1993;11:595–605.
2. Portera-Cailliau C, Sung CH, Nathans J, Adler R. Apoptotic photoreceptor cell death in mouse models of retinitis pigmentosa. *Proc Natl Acad Sci U S A*. 1994;91:974–978.
3. Sancho-Pelluz J, Arango-Gonzalez B, Kustermann S, et al. Photoreceptor cell death mechanisms in inherited retinal degeneration. *Mol Neurobiol*. 2008;38:253–269.
4. Wert KJ, Lin JH, Tsang SH. General pathophysiology in retinal degeneration. *Dev Ophthalmol*. 2014;53:33–43.
5. Chang B, Hawes NL, Pardue MT, et al. Two mouse retinal degenerations caused by missense mutations in the beta-subunit of rod cGMP phosphodiesterase gene. *Vision Res*. 2007;47:624–633.
6. Gargini C, Terzibasi E, Mazzoni F, Strettoi E. Retinal organization in the retinal degeneration 10 (rd10) mutant mouse: a morphological and ERG study. *J Comp Neurol*. 2007;500:222–238.
7. Barhoum R, Martinez-Navarrete G, Corrochano S, et al. Functional and structural modifications during retinal degeneration in the rd10 mouse. *Neuroscience*. 2008;155:698–713.
8. Faktorovich EG, Steinberg RH, Yasumura D, Matthes MT, LaVail MM. Photoreceptor degeneration in inherited retinal dystrophy delayed by basic fibroblast growth factor. *Nature*. 1990;347:83–86.
9. LaVail MM, Unoki K, Yasumura D, Matthes MT, Yancopoulos GD, Steinberg RH. Multiple growth factors, cytokines, and neurotrophins rescue photoreceptors from the damaging effects of constant light. *Proc Natl Acad Sci U S A*. 1992;89:11249–11253.
10. LaVail MM, Yasumura D, Matthes MT, et al. Protection of mouse photoreceptors by survival factors in retinal degenerations. *Invest Ophthalmol Vis Sci*. 1998;39:592–602.
11. Caffe AR, Soderpalm AK, Holmqvist I, van Veen T. A combination of CNTF and BDNF rescues rd photoreceptors but changes rod differentiation in the presence of RPE in retinal explants. *Invest Ophthalmol Vis Sci*. 2001;42:275–282.
12. Rivas MA, Vecino E. Animal models and different therapies for treatment of retinitis pigmentosa. *Histol Histopathol*. 2009;24:1295–1322.
13. El Sanharawi M, Kowalczuk L, Touchard E, Omri S, de Kozak Y, Behar-Cohen F. Protein delivery for retinal diseases: from basic considerations to clinical applications. *Prog Retin Eye Res*. 2010;29:443–465.
14. Bramall AN, Wright AF, Jacobson SG, McInnes RR. The genomic, biochemical, and cellular responses of the retina in inherited photoreceptor degenerations and prospects for the treatment of these disorders. *Annu Rev Neurosci*. 2010;33:441–472.
15. Kolomeyer AM, Zarbin MA. Trophic factors in the pathogenesis and therapy for retinal degenerative diseases. *Surv Ophthalmol*. 2014;59:134–165.
16. Cuenca N, Fernandez-Sanchez L, Campello L, et al. Cellular responses following retinal injuries and therapeutic approaches for neurodegenerative diseases. *Prog Retin Eye Res*. 2014;43:17–75.
17. Andrieu-Soler C, Aubert-Pouessel A, Doat M, et al. Intravitreous injection of PLGA microspheres encapsulating GDNF promotes the survival of photoreceptors in the rd1/rd1 mouse. *Mol Vis*. 2005;11:1002–1011.
18. Zeiss CJ, Allore HG, Towle V, Tao W. CNTF induces dose-dependent alterations in retinal morphology in normal and rcd-1 canine retina. *Exp Eye Res*. 2006;82:395–404.
19. Leveillard T, Fridlich R, Clerin E, et al. Therapeutic strategy for handling inherited retinal degenerations in a gene-independent manner using rod-derived cone viability factors. *C R Biol*. 2014;337:207–213.
20. Sanchez-Vallejo V, Benlloch-Navarro S, Lopez-Pedrajas R, Romero FJ, Miranda M. Neuroprotective actions of progesterone in an in vivo model of retinitis pigmentosa. *Pharmacol Res*. 2015;99:276–288.
21. Wyse Jackson AC, Roche SL, Byrne AM, Ruiz-Lopez AM, Cotter TG. Progesterone receptor signalling in retinal photoreceptor neuroprotection. *J Neurochem*. 2015;136:63–77.
22. Corrochano S, Barhoum R, Boya P, et al. Attenuation of vision loss and delay in apoptosis of photoreceptors induced by proinsulin in a mouse model of retinitis pigmentosa. *Invest Ophthalmol Vis Sci*. 2008;49:4188–4194.
23. Punzo C, Kornacker K, Cepko CL. Stimulation of the insulin/mTOR pathway delays cone death in a mouse model of retinitis pigmentosa. *Nat Neurosci*. 2009;12:44–52.

24. Fernandez-Sanchez L, Lax P, Isiegas C, et al. Proinsulin slows retinal degeneration and vision loss in the P23H rat model of retinitis pigmentosa. *Hum Gene Ther*. 2012;23:1290–1300.
25. de Pablo F, de la Rosa EJ. The developing CNS: a scenario for the action of proinsulin, insulin and insulin-like growth factors. *Trends Neurosci*. 1995;18:143–150.
26. Valenciano AI, Boya P, de la Rosa EJ. Early neural cell death: numbers and cues from the developing neuroretina. *Int J Dev Biol*. 2009;53:1515–1528.
27. de la Rosa EJ, de Pablo F. Proinsulin: from hormonal precursor to neuroprotective factor. *Front Mol Neurosci*. 2011;4:20.
28. Vergara MN, de la Rosa EJ, Canto-Soler MV. Focus on molecules: proinsulin in the eye: precursor or pioneer? *Exp Eye Res*. 2012;101:109–110.
29. Rong X, Yang S, Miao H, et al. Effects of erythropoietin-dextran microparticle-based PLGA/PLA microspheres on RGCs. *Invest Ophthalmol Vis Sci*. 2012;53:6025–6034.
30. Herrero-Vanrell R, Bravo-Osuna I, Andres-Guerrero V, Vicario-de-la-Torre M, Molina-Martinez IT. The potential of using biodegradable microspheres in retinal diseases and other intraocular pathologies. *Prog Retin Eye Res*. 2014;42:27–43.
31. Mao S, Xu J, Cai C, Germershaus O, Schaper A, Kissel T. Effect of WOW process parameters on morphology and burst release of FITC-dextran loaded PLGA microspheres. *Int J Pharm*. 2007;334:137–148.
32. Azvolinsky A. Gene therapy 'cure' for blindness wanes. *Nat Biotechnol*. 2015;33:678.
33. Chinskey ND, Besirli CG, Zacks DN. Retinal cell death and current strategies in retinal neuroprotection. *Curr Opin Ophthalmol*. 2014;25:228–233.
34. Jacobson SG, Cideciyan AV, Roman AJ, et al. Improvement and decline in vision with gene therapy in childhood blindness. *N Engl J Med*. 2015;372:1920–1926.
35. Jacobson SG, Cideciyan AV, Aguirre GD, et al. Improvement in vision: a new goal for treatment of hereditary retinal degenerations. *Expert Opin Orphan Drugs*. 2015;3:563–575.
36. Thanos C, Emerich D. Delivery of neurotrophic factors and therapeutic proteins for retinal diseases. *Expert Opin Biol Ther*. 2005;5:1443–1452.
37. Wen R, Tao W, Li Y, Sieving PA. CNTF and retina. *Prog Retin Eye Res*. 2012;31:136–151.
38. Imai H, Misra GP, Wu L, Janagam DR, Gardner TW, Lowe TL. Subconjunctivally implanted hydrogels for sustained insulin release to reduce retinal cell apoptosis in diabetic rats. *Invest Ophthalmol Vis Sci*. 2015;56:7839–7846.
39. Arroba AI, Alvarez-Lindo N, van Rooijen N, de la Rosa EJ. Microglia-mediated IGF-I neuroprotection in the rd10 mouse model of retinitis pigmentosa. *Invest Ophthalmol Vis Sci*. 2011;52:9124–9130.
40. Arroba AI, Alvarez-Lindo N, van Rooijen N, de la Rosa EJ. Microglia-Muller glia crosstalk in the rd10 mouse model of retinitis pigmentosa. *Adv Exp Med Biol*. 2014;801:373–379.
41. Phillips MJ, Walker TA, Choi HY, et al. Tauroursodeoxycholic acid preservation of photoreceptor structure and function in the rd10 mouse through postnatal day 30. *Invest Ophthalmol Vis Sci*. 2008;49:2148–2155.
42. Malaguarnera R, Sacco A, Voci C, Pandini G, Vigneri R, Belfiore A. Proinsulin binds with high affinity the insulin receptor isoform A and predominantly activates the mitogenic pathway. *Endocrinology*. 2012;153:2152–2163.
43. Reiter CE, Gardner TW. Functions of insulin and insulin receptor signaling in retina: possible implications for diabetic retinopathy. *Prog Retin Eye Res*. 2003;22:545–562.
44. Rodrigues M, Waldbillig RJ, Rajagopalan S, Hackett J, LeRoith D, Chader GJ. Retinal insulin receptors: localization using a polyclonal anti-insulin receptor antibody. *Brain Res*. 1988; 443:389–394.
45. Gosbell AD, Favilla I, Jablonski P. The location of insulin receptors in bovine retina and isolated retinal cells. *Clin Experiment Ophthalmol*. 2002;30:124–130.
46. Rajala A, Tanito M, Le YZ, Kahn CR, Rajala RV. Loss of neuroprotective survival signal in mice lacking insulin receptor gene in rod photoreceptor cells. *J Biol Chem*. 2008;283:19781–19792.
47. Valenciano AI, Corrochano S, de Pablo F, de la Villa P, de la Rosa EJ. Proinsulin/insulin is synthesized locally and prevents caspase- and cathepsin-mediated cell death in the embryonic mouse retina. *J Neurochem*. 2006;99:524–536.

Investigative Ophthalmology & Visual Science